



# Pillar[5]arene Based [1]rotaxane Systems With Redox-Responsive Host-Guest Property: Design, Synthesis and the Key Role of Chain Length

Runmiao Zhang<sup>1,2</sup>, Chenwei Wang<sup>1</sup>, Renhua Long<sup>1</sup>, Tingting Chen<sup>1\*</sup>, Chaoguo Yan<sup>2\*</sup> and Yong Yao<sup>1\*</sup>

<sup>1</sup> College of Chemistry, Nantong University, Nantong, China, <sup>2</sup> College of Chemistry, Yangzhou University, Yangzhou, China

## OPEN ACCESS

### Edited by:

De-Xian Wang,  
Institute of Chemistry (CAS), China

### Reviewed by:

Xiao-Yu Hu,  
Nanjing University of Aeronautics and  
Astronautics, China

Tangxin Xiao,  
Changzhou University, China

Haibo Yang,  
East China Normal University, China

### \*Correspondence:

Tingting Chen  
ttchen1980@126.com  
Chaoguo Yan  
cgyan@yzu.edu.cn  
Yong Yao  
yaoyong1986@ntu.edu.cn

### Specialty section:

This article was submitted to  
Supramolecular Chemistry,  
a section of the journal  
Frontiers in Chemistry

Received: 05 May 2019

Accepted: 02 July 2019

Published: 23 July 2019

### Citation:

Zhang R, Wang C, Long R, Chen T,  
Yan C and Yao Y (2019) Pillar[5]arene  
Based [1]rotaxane Systems With  
Redox-Responsive Host-Guest  
Property: Design, Synthesis and the  
Key Role of Chain Length.  
Front. Chem. 7:508.  
doi: 10.3389/fchem.2019.00508

Pillar[n]arenes are a new type of macrocyclic compounds, which were first reported in 2008 by Ogoshi. They not only have cylindrical, symmetrical, and rigid structures, but also have many advantages, including easy functionalization and rich host-guest properties. On the other hand, mechanically interlocked molecules (MIMs) exist extensively in nature which have been artificially synthesized and widely applied in the fields of nanotechnology and biology. Although pillar[5]arene-based MIMs have been investigated much over recent years, pillar[5]arene-based [1]rotaxanes are very limited. In this report, we synthesized a series of amide-linked pillar[5]arene-based [1]rotaxanes with ferrocene unit as the stopper. Under the catalysis of HOBT/EDCL, the mono-amido-functionalized pillar[5]arenes were amidated with ferrocene carboxylic acid to construct ferrocene-based [1]rotaxanes, respectively. The structure of the [1]rotaxanes were characterized by <sup>1</sup>H NMR, <sup>13</sup>C NMR, 2D NMR, mass spectroscopy, and single-crystal X-ray structural determination. In the experiment, the monofunctionalized pillar[5]arene was synthesized with a self-inclusion property, which allows for forming a pseudo-rotaxane. The key role is the length of the imine chain in this process. The formation of a rotaxane was realized through amidation of ferrocene dicarboxylic acid, which acted as a plug. In addition, due to the ferrocene units, the pillar[5]arene-based [1]rotaxanes perform electrochemically reversible property. Based on this nature, we hope these pillar[5]arene-based [1]rotaxanes can be applied in battery devices in the future.

**Keywords:** pillar[n]arenes, rotaxanes, electrochemically reversible, single-crystal X-ray, ferrocene

## INTRODUCTION

Mechanically interlocked molecules (MIMs) are a type of “star” molecule due to their beautiful and interesting architectures and wide applications in the area of biology and nanoscience (Bissell et al., 1994; Brouwer et al., 2001; Zhu and Chen, 2005; Crowley et al., 2009; Yonath, 2010; Zhang et al., 2011; Li et al., 2014; Wang et al., 2015, 2018). Among various MIMs, rotaxanes, which have dumbbell-like structures with a wheel sliding along an axle, have attracted great interest due to their wide application in preparation of artificial molecular machines (Green et al., 2007; Lewandowski et al., 2013; Zhang et al., 2013). [1]rotaxanes, whose wheels and axles are connected in one molecule

by covalent bonds, have a stable threaded form in both solution and solid state (Hiratani et al., 2004; Franchi et al., 2008; Li et al., 2012). However, the efficient synthesis of [1]rotaxanes is very difficult due to their subtle structure. To the best of our knowledge, there are very limited studies about the synthesis and properties of macrocycle based [1]rotaxanes. For example, Prof. Yang et al. prepared a functionalized [1]rotaxane and applied it to catalysis Knoevenagel reaction in  $\text{CHCl}_3$  (Du et al., 2017). Prof. Qu et al. fabricated a novel [1]rotaxane-based molecular motion modified with ferrocene groups (Li et al., 2012).

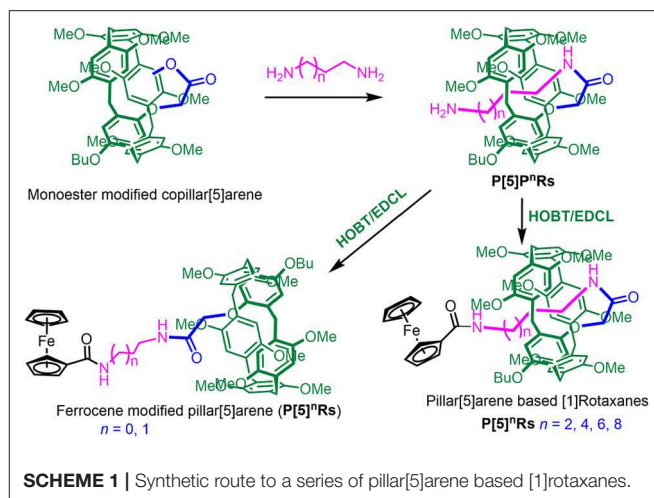
Pillar[ $n$ ]arenes (Ogoshi et al., 2008; Cragg and Sharma, 2012; Xue et al., 2012; Si et al., 2015; Wang et al., 2015, 2016; Sun et al., 2018; Xiao and Wang, 2018; Xiao et al., 2019a,b), which are the newest host compounds in supramolecular chemistry after crown ethers (Liu et al., 2017; Yoo et al., 2019), cyclodextrins (Fu et al., 2019), calix[ $n$ ]arenes (Dalgarno et al., 2007), and cucurbiturils (Murray et al., 2017), have attracted extensive investigations due to their pillar-like topology, rigid structures, electron-rich cavities, and rich host-guest properties (Song and Yang, 2015; Li et al., 2019; Wang et al., 2019). Up to now, pillar[ $n$ ]arene-based pseudo[1]rotaxanes with ammonium units, urea groups, pyridinium salt or biotin units as the axles have been investigated a lot (Strutt et al., 2012; Ni et al., 2014; Wu et al., 2015), but the further formation of [1]rotaxanes is difficult due to the lack of reactivity with stoppers. With the constant efforts by scientists, several examples of pillar[ $n$ ]arene-based [1]rotaxanes have been fabricated successfully. For example, Prof. Xue et al. combined C-H- $\pi$  and ion-pair interactions to construct a pillar[5]arene-based [1]rotaxane in a yield of 73% (Xia and Xue, 2014). Prof. Yan et al. prepared a series of pillar[5]arene-based [1]rotaxanes from mono-amide-modified pillar[5]arenes with different lengths of the axles (Han et al., 2016).

Herein, we designed and synthesized a series of pillar[5]arene-based [1]rotaxanes with *N*-aminoalkyl amides as the axles and ferrocenecarboxylic acid as the stoppers through a method called “threading-followed-by-stoppering” (Cao et al., 2000). Self-included pillar[5]arene-based pseudo[1]-rotaxanes **P[5]<sup>n</sup>PRs** were prepared from monoester modified copillar[5]arene according previous research. Then pillar[5]arene based [1]rotaxanes **P[5]<sup>n</sup>Rs** were directly obtained by **P[5]<sup>n</sup>PRs** reacted with ferrocenecarboxylic acid as the stopper under the catalysis of HOBT/EDCL. Importantly, we found that the length of *N*-aminoalkyl chains play a key role in the formation of [1]rotaxanes—only when the number of carbon on the *N*-aminoalkyl chains larger than three can it form [1]rotaxanes. Moreover, these [1]rotaxanes showed electrochemically reversible properties due to the ferrocene unit on them.

## MATERIALS AND METHODS

### Synthesis of Pillar[5]arenes-Based [1]rotaxanes and Mono-ferrocene Modified Pillar[5]arene

Based on previous work (Han et al., 2016), **P[5]<sup>n</sup>PRs** were obtained directly from mono-ester modified pillar[5]arene



(**Scheme 1**). Then, **P[5]<sup>n</sup>PRs** and mono-ferrocene modified pillar[5]arene were successfully synthesized by **P[5]<sup>n</sup>PRs** reacted with ferrocene-carboxylic acid as the stopper under the catalysis of HOBT/EDCL. We take when  $n = 4$  as a model reaction, **P[5]<sup>4</sup>PR** (0.203 g, 0.2 mmol), ferrocenecarboxylic acid (0.052 g, 0.2 mmol), HOBT(0.038 g, 0.25 mmol), and EDCL (0.055 g, 0.25 mmol) were stirred in 10 mL dry  $\text{CHCl}_3$  over night at room temperature. The reaction solvent was evaporated and the residue was purified by flash column chromatography on silica gel ( $\text{CH}_2\text{Cl}_2/\text{CH}_3\text{OH}$ ,  $v/v$  15:1) to give **P[5]<sup>4</sup>R** as a yellow solid (0.195 g). Other **P[5]<sup>n</sup>PRs** and mono-ferrocene modified pillar[5]arene were prepared with the similar method (**Scheme 1**).

### P[5]<sup>2</sup>R

Yellow solid, 78.6%, m.p. 106.9–108.5°C;  $^1\text{H}$  NMR (400 MHz,  $\text{CDCl}_3$ )  $\delta$ : 7.05–6.89 (m, 7 H, ArH), 6.84 (d,  $J = 2.5$  Hz, 1 H, ArH), 6.80 (s, 1 H, ArH), 6.60 (s, 1 H, ArH), 5.04–4.81 (m, 4 H,  $\text{CH}_2$ ), 4.50 (s, 2 H, ArH), 4.39 (s, 2 H, ArH), 4.24 (d,  $J = 2.5$  Hz, 5 H, ArH), 4.05–3.95 (m, 2 H,  $\text{CH}_2$ ), 3.95–3.60 (m, 32 H, 24  $\text{CH}_3$ , 8  $\text{CH}_2$ ), 3.54 (s, 4 H,  $\text{CH}_2$ ), 1.80 (d,  $J = 8.1$  Hz, 2 H,  $\text{CH}_2$ ), 1.55 (d,  $J = 7.6$  Hz, 2 H,  $\text{CH}_2$ ), 1.02 (d,  $J = 7.5$  Hz, 3 H,  $\text{CH}_2$ ), -1.90 (d,  $J = 50.7$  Hz, 2 H,  $\text{CH}_2$ ), -2.19 (d,  $J = 42.0$  Hz, 2 H,  $\text{CH}_2$ );  $^{13}\text{C}$  NMR (101 MHz,  $\text{CDCl}_3$ ) (**Figure S9**)  $\delta = 169.0, 168.9, 168.9, 166.7, 151.4, 150.6, 150.6, 150.5, 150.3, 150.3, 150.2, 150.2, 150.2, 150.1, 150.1, 149.7, 148.9, 129.8, 128.8, 128.8, 128.5, 128.4, 128.0, 127.7, 126.6, 126.4, 119.0, 115.5, 113.8, 113.7, 113.5, 113.4, 113.0, 112.9, 112.5, 112.5, 112.4, 112.4, 77.3, 71.8, 71.8, 69.9, 69.9, 69.9, 69.6, 68.5, 67.8, 66.0, 57.0, 56.4, 56.0, 55.8, 55.6, 55.5, 55.3, 55.2, 39.5, 37.5, 31.9, 31.7, 29.8, 29.7, 28.6, 28.5, 27.2, 23.2, 22.3, 22.3, 19.5, 14.1; MS (m/z): HRMS (ESI) Calcd. for  $\text{C}_{64}\text{H}_{75}\text{FeN}_2\text{O}_{12}^+$  ( $[\text{M} + \text{H}]^+$ ): 1119.4671, found: 1119.4669 (**Figure S10**).$

### P[5]<sup>4</sup>R

Yellow solid, 42.9%, m.p. 107.4–109.2°C;  $^1\text{H}$  NMR (400 MHz,  $\text{CDCl}_3$ )  $\delta$  7.02–6.76 (m, 10 H, ArH), 5.67 (s, 1 H, NH), 5.26 (s, 1 H, NH), 4.75 (s, 2 H,  $\text{CH}_2$ ), 4.59 (s, 2 H, ArH), 4.40 (s, 2 H, ArH), 4.24 (d,  $J = 2.4$  Hz, 5 H, ArH), 4.05–3.54 (m, 36 H,

24 OCH<sub>3</sub>, 12 CH<sub>2</sub>), 2.72–2.47 (m, 4 H, CH<sub>2</sub>), 1.76 (dd,  $J = 15.2, 8.0$  Hz, 2 H, CH<sub>2</sub>), 1.52 (q,  $J = 7.6$  Hz, 2 H, CH<sub>2</sub>), 0.96 (t,  $J = 7.6$  Hz, 3 H, CH<sub>3</sub>), -0.18 (s, 2 H, CH<sub>2</sub>), -0.90 (s, 1 H, CH<sub>2</sub>), -1.09 (s, 1 H, CH<sub>2</sub>), -1.61 (d,  $J = 23.6$  Hz, 2 H, CH<sub>2</sub>), -2.21 (s, 2 H, CH<sub>2</sub>); <sup>13</sup>C NMR (101 MHz, CDCl<sub>3</sub>) (Figure S13)  $\delta = 169.25, 167.51, 150.91, 150.73, 150.56, 150.45, 150.40, 150.36, 150.32, 150.21, 150.12, 147.21, 129.75, 129.29, 128.75, 128.48, 128.45, 128.19, 127.87, 127.82, 127.05, 115.82, 115.08, 114.71, 114.43, 114.00, 112.80, 112.78, 112.73, 112.23, 70.21, 68.88, 68.09, 67.81, 65.85, 56.83, 56.44, 56.29, 56.26, 56.08, 55.48, 55.43, 55.31, 55.10, 39.73, 37.87, 31.95, 30.15, 29.36, 28.89, 28.60, 28.44, 26.37, 24.41, 23.25, 19.57, 14.06$ ; HRMS (ESI) Calcd. for C<sub>66</sub>H<sub>79</sub>FeN<sub>2</sub>O<sub>12</sub><sup>+</sup> ([M + H]<sup>+</sup>): 1147.4981, found: 1147.4982 (Figure S14).

### P[5]<sup>6</sup>R

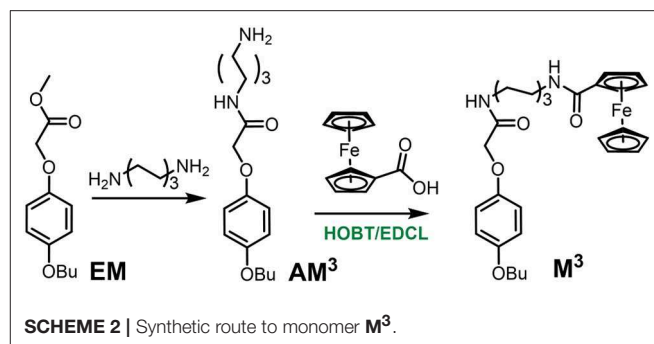
Yellow solid, 38.9%, m.p. 109.9–112.1°C; <sup>1</sup>H NMR (400 MHz, CDCl<sub>3</sub>)  $\delta$ : 6.98–6.70 (m, 10 H, ArH), 5.85 (s, 1 H, NH), 5.18 (s, 1 H, NH), 4.72 (s, 2 H, CH<sub>2</sub>), 4.58 (s, 2 H, ArH), 4.39 (s, 2 H, ArH), 4.24 (s, 5 H, ArH), 4.00–3.59 (m, 36 H, 24 OCH<sub>3</sub>, 12 CH<sub>2</sub>), 3.42 (s, 2 H, CH<sub>2</sub>), 3.29 (s, 2 H, CH<sub>2</sub>), 1.86–1.79 (m, 2 H, CH<sub>2</sub>), 1.60 (q,  $J = 7.6$  Hz, 2 H, CH<sub>2</sub>), 1.35 (s, 2 H, CH<sub>2</sub>), 1.03 (t,  $J = 6.3$  Hz, 3 H, CH<sub>3</sub>), 0.72 (s, 2 H, CH<sub>2</sub>), -0.17 (s, 2 H, CH<sub>2</sub>), -1.11 (s, 1 H, CH<sub>2</sub>), -1.25 (s, 1 H, CH<sub>2</sub>), -1.50 (s, 2 H, CH<sub>2</sub>), -2.32 (s, 2 H, CH<sub>2</sub>); <sup>13</sup>C NMR (101 MHz, CDCl<sub>3</sub>) (Figure S17)  $\delta = 169.86, 150.81, 150.52, 150.48, 150.30, 150.20, 149.99, 129.41, 129.05, 128.35, 128.24, 128.09, 127.85, 127.34, 115.04, 114.18, 114.13, 113.70, 112.76, 112.33, 77.34, 70.43, 69.72, 68.19, 68.11, 55.99, 55.69, 55.46, 55.39, 55.29, 55.12, 40.01, 37.99, 32.02, 30.71, 30.11, 29.27, 29.01, 28.89, 28.62, 28.41, 28.27, 27.72, 19.65, 14.14$ ; MS (m/z): HRMS (ESI) Calcd. for C<sub>68</sub>H<sub>83</sub>FeN<sub>2</sub>O<sub>12</sub><sup>+</sup> ([M + H]<sup>+</sup>): 1175.5294, found: 1175.5295 (Figure S18).

### P[5]<sup>8</sup>R

Yellow solid, 25.9%, m.p. 114.6–116.8°C; <sup>1</sup>H NMR (400 MHz, CDCl<sub>3</sub>)  $\delta$ : 6.95–6.80 (m, 9 H, ArH), 6.71 (s, 1 H, ArH), 5.23 (s, 1 H, NH), 5.02 (s, 1 H, NH), 4.68 (t,  $J = 1.9$  Hz, 2 H, CH<sub>2</sub>), 4.56 (s, 2 H, ArH), 4.37 (t,  $J = 2.0$  Hz, 2 H, ArH), 4.22 (s, 5 H, ArH), 3.92–3.63 (m, 36 H, 24 OCH<sub>3</sub>, 12 CH<sub>2</sub>), 3.42 (q,  $J = 7.0$  Hz, 2 H, CH<sub>2</sub>), 2.41 (s, 2 H, CH<sub>2</sub>), 1.88–1.79 (m, 2 H, CH<sub>2</sub>), 1.62 (td,  $J = 7.4, 2.6$  Hz, 4 H, CH<sub>2</sub>), 1.37 (p,  $J = 7.7$  Hz, 2 H, CH<sub>2</sub>), 1.20 (t,  $J = 7.9$  Hz, 2 H, CH<sub>2</sub>), 1.04 (t,  $J = 7.4$  Hz, 3 H, CH<sub>3</sub>), 0.80 (s, 2 H, CH<sub>2</sub>), -0.05 (s, 2 H, CH<sub>2</sub>), -1.34 (s, 4 H, CH<sub>2</sub>), -2.38 (s, 2 H, CH<sub>2</sub>); <sup>13</sup>C NMR (101 MHz, CDCl<sub>3</sub>) (Figure S21)  $\delta = 170.09, 167.19, 150.80, 150.37, 150.24, 150.12, 150.06, 149.95, 146.97, 129.40, 129.01, 128.32, 128.20, 128.11, 127.94, 127.84, 127.83, 127.08, 114.73, 113.92, 113.58, 113.25, 112.73, 112.42, 76.31, 70.43, 69.72, 68.00, 67.82, 55.48, 55.45, 55.36, 55.32, 55.13, 39.72, 38.02, 32.05, 30.96, 30.66, 30.60, 30.21, 29.64, 29.26, 28.83, 28.76, 28.64, 28.22, 27.94, 19.65, 14.17$ ; IR (KBr)  $\nu$ : 3410, 2932, 2854, 1681, 1499, 1465, 1399, 1295, 1213, 1104, 1047, 929, 879, 855, 774, 704, 647 cm<sup>-1</sup>; MS (m/z): HRMS (ESI) Calcd. for C<sub>70</sub>H<sub>87</sub>FeN<sub>2</sub>O<sub>12</sub><sup>+</sup> ([M + H]<sup>+</sup>): 1203.5602, found: 1203.5508 (Figure S22).

### Mono-ferrocene Modified Pillar[5]arene P[5]<sup>0</sup>R

Yellow solid, 78.6%, m.p. 104.4–106.2°C; <sup>1</sup>H NMR (400 MHz, CDCl<sub>3</sub>) (Figure S1)  $\delta$ : 6.78–6.82 (m, 4 H, ArH), 6.76 (d,  $J =$



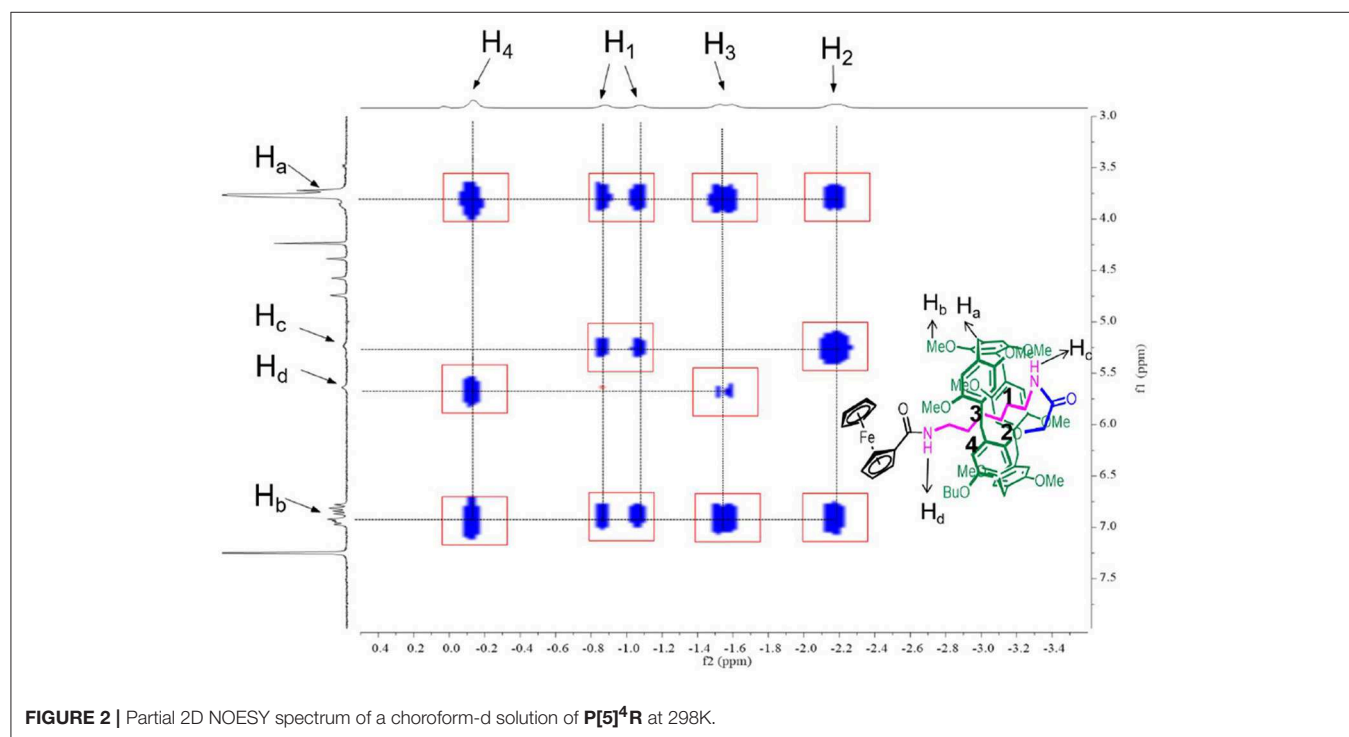
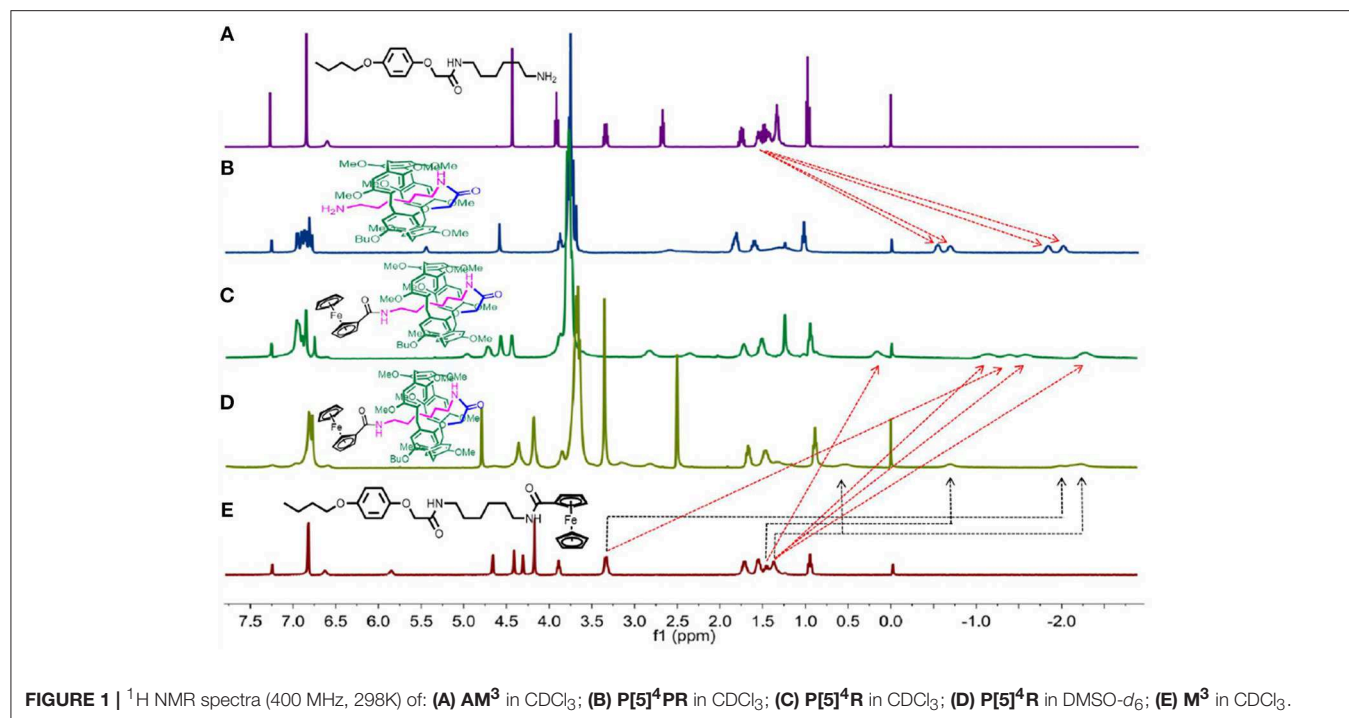
2.7 Hz, 2 H, ArH), 6.70 (s, 1 H, ArH), 6.65 (s, 1 H, ArH), 4.68 (t,  $J = 1.9$  Hz, 2 H, ArH), 4.37 (s, 2 H, CH<sub>2</sub>), 4.32 (t,  $J = 1.9$  Hz, 2 H, ArH), 4.19 (s, 5 H, ArH), 3.88 (t,  $J = 6.4$  Hz, 2 H, CH<sub>2</sub>), 3.85–3.62 (m, 28 H, 24 OCH<sub>3</sub>, 4 CH<sub>2</sub>), 3.60 (s, 3 H, CH<sub>2</sub>), 3.56 (s, 3 H, CH<sub>2</sub>), 3.24 (s, 2 H, CH<sub>2</sub>), 3.11 (s, 2 H, CH<sub>2</sub>), 1.72–1.82 (m, 2 H, CH<sub>2</sub>), 1.53 (h,  $J = 7.4$  Hz, 2 H, CH<sub>2</sub>), 0.97 (t,  $J = 7.4$  Hz, 3 H, CH<sub>3</sub>); <sup>13</sup>C NMR (101 MHz, CDCl<sub>3</sub>) (Figure S2)  $\delta = 170.70, 151.19, 150.87, 150.82, 150.77, 150.76, 150.69, 150.66, 148.15, 129.28, 129.23, 128.62, 128.46, 128.36, 128.08, 127.84, 127.72, 115.41, 115.34, 114.37, 114.31, 114.06, 114.03, 113.97, 113.90, 113.79, 76.13, 70.33, 69.70, 68.37, 68.24, 67.67, 56.68, 56.17, 56.06, 55.91, 55.87, 55.80, 55.77, 41.21, 38.87, 31.80, 30.21, 29.70, 29.64, 28.76, 19.50, 13.96$ ; MS (m/z): HRMS (ESI) Calcd. for C<sub>62</sub>H<sub>71</sub>FeN<sub>2</sub>O<sub>12</sub><sup>+</sup> ([M + H]<sup>+</sup>): 1091.4357, found: 1091.4356 (Figure S3).

### P[5]<sup>1</sup>R

Yellow solid, 71.9 %, m.p. 105.6–107.3°C; <sup>1</sup>H NMR (400 MHz, CDCl<sub>3</sub>) (Figure S5)  $\delta$ : 6.75–6.98 (m, 10 H, ArH), 6.60 (s, 2 H, NH), 4.77 (t,  $J = 2.0$  Hz, 2 H, ArH), 4.39 (s, 2 H, CH<sub>2</sub>), 4.34 (t,  $J = 1.9$  Hz, 2 H, ArH), 4.20 (s, 5 H, ArH), 3.46–3.97 (m, 36 H, 24 OCH<sub>3</sub>, 12 CH<sub>2</sub>), 1.81 (p,  $J = 6.9$  Hz, 2 H, CH<sub>2</sub>), 1.68 (s, 2 H, CH<sub>2</sub>), 1.56 (q,  $J = 7.5$  Hz, CH<sub>2</sub>), 1.01 (t,  $J = 7.4$  Hz, 3 H, CH<sub>3</sub>); <sup>13</sup>C NMR (101 MHz, CDCl<sub>3</sub>) (Figure S6)  $\delta = 150.7, 150.6, 150.4, 148.6, 128.8, 128.3, 128.1, 128.1, 114.6, 114.6, 114.5, 114.4, 113.7, 113.4, 113.3, 113.2, 70.0, 70.0, 69.6, 68.2, 66.9, 56.2, 56.2, 56.2, 55.9, 55.9, 55.7, 55.5, 39.4, 35.7, 34.8, 31.9, 29.7, 29.4, 19.5, 14.1$ ; MS (m/z): HRMS (ESI) Calcd. for C<sub>63</sub>H<sub>73</sub>FeN<sub>2</sub>O<sub>12</sub><sup>+</sup> ([M + H]<sup>+</sup>): 1105.4512, found: 1105.4513 (Figure S7).

### Synthesis of Monomer M<sup>3</sup>

AM<sup>3</sup> was obtained from a previous report. Then the monomer M<sup>3</sup> was synthesized from AM<sup>3</sup> (Figure S23) and ferrocene-carboxylic acid with BOBT and EDCL as the catalyst (Scheme 2). AM<sup>3</sup> (0.08 g, 0.25 mmol), ferrocene-carboxylic acid (0.057 g, 0.25 mmol), HOBT (0.054 g, 0.40 mmol), and EDCL (0.076 g, 0.40 mmol) were stirred in 15 mL dry CHCl<sub>3</sub> over night at room temperature. The reaction solvent was evaporated and the residue was purified by flash column chromatography on silica gel (CH<sub>2</sub>Cl<sub>2</sub>/CH<sub>3</sub>OH,  $v/v$  25:1) to give M<sup>3</sup> as a yellow solid (0.031 g). <sup>1</sup>H NMR (400 MHz, CDCl<sub>3</sub>) (Figure S24)  $\delta$ : 6.84 (s, 4 H, ArH), 6.65 (s, 1 H, NH), 5.87 (s, 1 H,



NH), 4.68 (s, 2H,  $\text{CH}_2$ ), 4.44 (s, 2H, ArH), 4.33 (s, 2H, ArH), 4.19 (s, 5H, ArH), 3.91 (t,  $J = 5.8$  Hz, 2H,  $\text{CH}_2$ ), 3.36 (d,  $J = 6.2$  Hz, 4H,  $\text{CH}_2$ ), 1.80–1.68 (m, 4H,  $\text{CH}_2$ ), 1.58 (d,  $J = 5.9$  Hz, 4H,  $\text{CH}_2$ ), 1.48 (dd,  $J = 14.6$ , 7.1 Hz, 2H,  $\text{CH}_2$ ), 1.39 (s, 2H,  $\text{CH}_2$ ), 0.97 (t,  $J = 6.9$  Hz, 3H,  $\text{CH}_3$ ).

## MATERIALS

All reactions were performed in atmosphere unless noted. All reagents were commercially available and used as supplied without further purification. NMR spectra were collected on either a Bruker AVIII-400 MHz spectrometer or a Bruker AV-600

MHz spectrometer with internal standard tetramethylsilane (TMS) and signals as internal references, and the chemical shifts ( $\delta$ ) were expressed in ppm. High-resolution Mass (ESI) spectra were obtained with a Bruker Micro-TOF spectrometer. X-ray data were collected on a Bruker Smart APEX-2 CCD diffractometer.

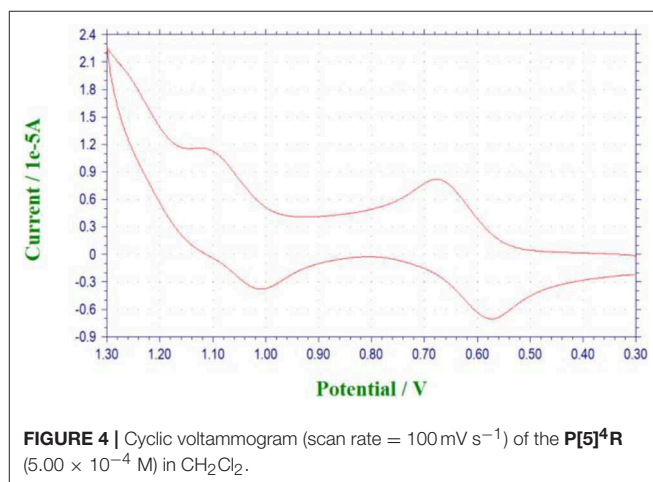
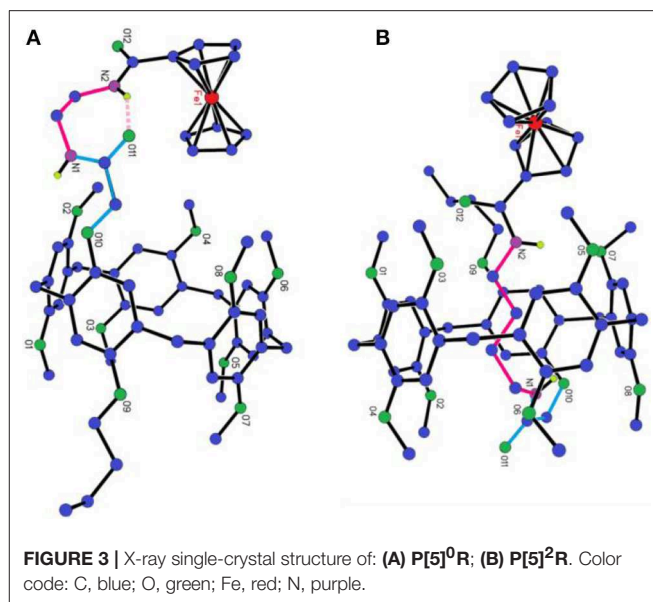
## RESULTS AND DISCUSSION

### $^1\text{H}$ NMR Investigation

The  $^1\text{H}$  NMR spectra of  $\text{AM}^3$  and  $\text{P}[5]^4\text{PR}$  were taken into consideration first. As shown in **Figure 1B**, the chemical shift of four groups of peaks shift below 0 ppm field, indicating that the alkyl chain penetrated into the cavity of pillar[5]arene to form either pseudo[1] rotaxane or [c2]daisy chain (Du et al., 2017). Then  $\text{P}[5]^4\text{R}$  was prepared from  $\text{P}[5]^4\text{PR}$  reacted with ferrocenecarboxylic acid as the stopper.  $^1\text{H}$  NMR spectra of monomer  $\text{M}^3$  and [1] rotaxane  $\text{P}[5]^4\text{R}$  in  $\text{CDCl}_3$  at 293 K are shown in **Figure 1** (spectra c and e). Compared with  $\text{M}^3$ , we found that the signals of protons on the alkyl chain attaching onto the pillar[5]arene platform shifted upfield obviously due to the shielding effect (**Figure 1C**). Then we used a polar solvent,  $\text{DMSO}-d_6$ , for  $^1\text{H}$  NMR investigations to confirm the formation of [1] rotaxane. In  $\text{DMSO}-d_6$ , we also found that the signals of protons on the alkyl chains upfield were below 0 ppm due to the shielding effect (**Figure 1D**), which indicated the formation of a mechanically interlocked structure (Dong et al., 2014). The  $^1\text{H}$  NMR of  $\text{P}[5]^2\text{R}$ ,  $\text{P}[5]^4\text{R}$ ,  $\text{P}[5]^6\text{R}$ ,  $\text{P}[5]^8\text{R}$  all showed several groups of protons on the alkyl chains upfield obviously (**Figures S8, S12, S16, S20**), and the formation of [1] rotaxanes was also confirmed. However, the  $^1\text{H}$  NMR of  $\text{P}[5]^0\text{R}$  and  $\text{P}[5]^1\text{R}$  showed no signal below 0 ppm, indicating the side-chain stayed outside of the cavity of the pillar[5]arene platform (**Figures S1, S5**). The reason for this phenomenon is due to the relatively short length of the axle (only two or three  $\text{CH}_2$  groups) of  $\text{P}[5]^0\text{R}$ , and  $\text{P}[5]^1\text{R}$ , which was not able to allow the large ferrocene group to connect it from the cavity. Thus, the amino-group of the side-chain of  $\text{P}[5]^0\text{PR}$  (or  $\text{P}[5]^1\text{PR}$ ) stayed outside of the cavity and was then reacted with ferrocene-carboxylic acid to obtain free form  $\text{P}[5]^0\text{R}$  (or  $\text{P}[5]^1\text{R}$ ). Furthermore, the temperature-dependent  $^1\text{H}$  NMR of  $\text{P}[5]^4\text{R}$  showed that the peaks became broad as the temperature increased, indicating the chain in the cavity (**Figures S15, S19, S26**).

### 2D NOESY Studies

The formation of [1]rotaxane was then confirmed by 2D Nuclear Overhauser Effect Spectroscopy (NOESY). Here we also take  $\text{P}[5]^4\text{R}$  as the model compound. As shown in **Figure 2**, the hydrogens of the alkyl chain on  $\text{P}[5]^4\text{R}$  were close to the pillar[5]arene platform because  $\text{H}_{1-4}$  showed strong correlation with  $\text{H}_a$  and  $\text{H}_b$ , indicating that the alkyl chain was in close proximity to the cavity. The  $-\text{NH}-$  group  $\text{H}_c$  is close to  $\text{H}_{1-2}$  while  $\text{H}_d$  is close to  $\text{H}_{3-4}$ . Furthermore,  $\text{ArH}-3$  from the ferrocene group showed space correction to the hydrogen- $-\text{OCH}_3$  and  $-\text{OCH}_2-$  on the pillar[5]arene platform (**Data Sheets 1-4**).



### Single Crystal Structures

The direct evidence for the formation of [1] rotaxanes only when the length of axle longer than three  $\text{CH}_2$  groups is from single crystal investigation. As shown in **Figure 3A** and **Figure S4**, the whole side chain of  $\text{P}[5]^0\text{R}$  stayed outside of the cavity of pillar[5]arene. It should be pointed that we observed hydrogen bonding between the hydrogen atom of the amine group and the oxygen atom of carbonyl group (**Figure 3A**, pink dash line). However, for  $\text{P}[5]^2\text{R}$ , we can clearly see that the alkyl chain penetrated into the cavity of pillar[5]arene to form a [1] rotaxane (**Figure 3B** and **Figure S11**). The  $\text{C}-\text{H}\cdots\pi$  interactions and  $\text{C}-\text{H}\cdots\text{O}$  interactions were the driving forces for the formation of [1] rotaxane.

### Cyclic Voltammetry Investigation

With the [1]rotaxanes in hand, we then investigated their reversible redox property by electrochemistry methods. Take  $\text{P}[5]^4\text{R}$  as an example, in cyclic voltammetry (CV) experiment (**Figure 4**), the cyclic voltammogram was quasi-reversible with

nearly equal  $i_{pa}$  and  $i_{pc}$ , in which the potential difference  $\Delta E_p$  was around 0.090 V. Compared with ferrocene,  $P[5]^4R$  has a larger half wave potential ( $E_{1/2} = 612$  mV). Further study showed that the free state  $P[5]^0R$  has the similar redox property with  $P[5]^4R$  due to the same ferrocene unit (Figure S25).

## CONCLUSIONS

In this paper, we synthesized a series of amide-linked pillar[5]arene-based [1]rotaxanes with ferrocene unit as the stopper. Under the catalysis of HOBT/EDCL, the mono-amido-functionalized pillar[5]arenes were amidated with ferrocene carboxylic acid, to constructed ferrocene-based [1]rotaxanes, respectively. The structure of the [1]rotaxanes were characterized by  $^1H$  NMR,  $^{13}C$  NMR, 2D NMR, mass spectroscopy and single-crystal X-ray structural determination. In the formation of [1]rotaxane, the key role is the length of the alkyl chain in this process, and only when the number of C on the alkyl chain is larger than three can the formation of [1]rotaxane occur. In addition, due to the ferrocene units, the pillar[5]arene-based [1]rotaxanes display electrochemically reversible properties. Based on this nature, we hope these pillar[5]arene-based [1]rotaxanes can be applied in battery devices in future.

## REFERENCES

- Bissell, S. A., Córdova, E., Kaifer, A. E., and Stoddart, J. F. (1994). A chemically and electrochemically switchable molecular shuttle. *Nature* 369, 133–136. doi: 10.1038/369133a0
- Brouwer, A. M., Frochot, C., Gatti, F. G., Leigh, D. A., Mottier, L., Paolucci, F., et al. (2001). Reversible translation motion in a hydrogen-bonded molecular shuttle. *Science* 291, 2124–2128. doi: 10.1126/science.1057886
- Cao, J., Fyfe, M. C., Stoddart, J. F., Cousins, G. R., and Glink, P. T. (2000). Molecular shuttles by the protecting group approach. *J. Org. Chem.* 65, 1937–1946. doi: 10.1021/jo991397w
- Cragg, P. J., and Sharma, K. (2012). Pillar[5]arene: fascinating cyclophanes with a bright future. *Chem. Soc. Rev.* 41, 597–607. doi: 10.1039/C1CS15164A
- Crowley, J. D., Goldup, S. M., Lee, A.-L., Leigh, D. A., and McBurney, R. T. (2009). Active metal template synthesis of rotaxanes, catenanes and molecular shuttles. *Chem. Soc. Rev.* 38, 1530–1541. doi: 10.1039/b804243h
- Dalgarno, S. J., Thallapally, P. K., Barbour, L. J., and Atwood, J. L. (2007). Engineering void space in organic van der Waals crystals: calixarenes lead the way. *Chem. Soc. Rev.* 36, 236–245. doi: 10.1039/b606047c
- Dong, S., Yuan, J., and Huang, F. (2014). A pillar[5]arene/imidazolium [2]rotaxane: solvent- and thermo-driven molecular motions and supramolecular gel formation. *Chem. Sci.* 5, 247–252. doi: 10.1039/C3SC52481G
- Du, X.-S., Wang, C.-Y., Jia, Q., Deng, R., Tian, H.-S., Zhang, H.-Y., et al. (2017). Pillar[5]arene-based [1]rotaxane: high-yield synthesis, characterization and application in Knoevenagel reaction. *Chem. Comm.* 53, 5326–5329. doi: 10.1039/C7CC02364B
- Franchi, P., Fani, M., Mezzina, E., and Lucarini, M. (2008). Increasing the persistency of stable free-radicals: synthesis and characterization of a nitroxide based [1]rotaxane. *Org. Lett.* 10, 1901–1904. doi: 10.1021/ol800405b
- Fu, G.-G., Chen, Y., Yu, Q., and Liu, Y. (2019). A tumor-targeting Ru/polysaccharide/protein supramolecular assembly with high photodynamic therapy ability. *Chem. Comm.* 55, 3148–3151. doi: 10.1039/C8CC09964B

## DATA AVAILABILITY

The raw data supporting the conclusions of this manuscript will be made available by the authors, without undue reservation, to any qualified researcher.

## AUTHOR CONTRIBUTIONS

RZ prepared all the pillar[5]arene-based [1]rotaxanes. CW and RL prepared the monomer  $M^3$ . TC and CY analyzed the data. YY analyzed the data and wrote the paper.

## ACKNOWLEDGMENTS

This work was supported by the National Natural Science Foundation of China (21801139), Natural Science Foundation of Jiangsu Province (BK20180942), the Natural Science Foundation of Nantong University for High-Level Talent (03083004), and the Large Instruments Open Foundation of Nantong University (KFJN1814).

## SUPPLEMENTARY MATERIAL

The Supplementary Material for this article can be found online at: <https://www.frontiersin.org/articles/10.3389/fchem.2019.00508/full#supplementary-material>

- Green, J. E., Choi, J. W., Boukai, A., Bunimovich, Y., Johnston-Halperin, E., Delonno, E., et al. (2007). A 160-kilobit molecular electronic memory patterned at  $10^{11}$  bits per square centimetre. *Nature* 445, 414–417. doi: 10.1038/nature05462
- Han, Y., Huo, G.-F., Sun, J., Xie, J., Yan, C.-G., Zhao, Y., et al. (2016). Formation of a series of stable pillar[5]arene-based pseudo[1]rotaxanes and their [1]rotaxanes in the crystal state. *Sci. Rep.* 6:28748. doi: 10.1038/srep28748
- Hiratani, K., Kaneyama, M., Nagawa, Y., Koyama, E., and Kanosato, M. (2004). Synthesis of [1]rotaxane via covalent bond formation and its unidirectional fluorescent response by energy transfer in the presence of lithium ion. *J. Am. Chem. Soc.* 126, 13568–13569. doi: 10.1021/ja046929r
- Lewandowski, B., De Bo, G. D., Ward, J. W., Pappmeyer, M., Kuschel, S., Aldegunde, M. J., et al. (2013). Sequence-specific peptide synthesis by an artificial small-molecule machine. *Science* 339, 189–193. doi: 10.1126/science.1229753
- Li, B., Wang, B., Huang, X., Dai, L., Cui, L., Li, J., et al. (2019). Terphen[n]arenes and quaterphen[n]arenes ( $n = 3-6$ ): one-pot synthesis, self-assembly into supramolecular gel, and iodine capture. *Angew. Chem.* 58, 3885–3889. doi: 10.1002/anie.201813972
- Li, H., Zhang, H., Zhang, Q., Zhang, Q.-W., and Qu, D.-H. (2012). A switchable ferrocene-based [1]rotaxane with an electrochemical signal output. *Org. Lett.* 14, 5900–5903. doi: 10.1021/ol302826g
- Li, Z.-Y., Zhang, Y., Zhang, C.-W., Chen, L.-J., Wang, C., Tan, H., et al. (2014). Cross-linked supramolecular polymer gels constructed from discrete multi-pillar[5]arene metallacycles and their multiple stimuli-responsive behavior. *J. Am. Chem. Soc.* 136, 8577–8589. doi: 10.1021/ja413047r
- Liu, Z., Nalluri, S. K. M., and Stoddart, J. F. (2017). Surveying macrocyclic chemistry: from flexible crown ethers to rigid cyclophanes. *Chem. Soc. Rev.* 46, 2459–2478. doi: 10.1039/C7CS00185A
- Murray, J., Kim, K., Ogoshi, T., Yao, W., and Gibb, B. C. (2017). The aqueous supramolecular chemistry of cucubit[n]urils, pillar[n]arenes and deep-cavity cavitands. *Chem. Soc. Rev.* 46, 2479–2496. doi: 10.1039/C7CS00095B

- Ni, M., Hu, X.-Y., Jiang, J., and Wang, L. (2014). The self-complexation of mono-urea-functionalized pillar[5]arenes with abnormal urea behaviors. *Chem. Comm.* 50, 1317–1319. doi: 10.1039/C3CC47823H
- Ogoshi, T., Kanai, S., Fujinami, S., Yamagishi, T.-A., and Nakamoto, Y. (2008). Para-Bridged symmetrical pillar[5]arenes: their lewis acid catalyzed synthesis and host-guest property. *J. Am. Chem. Soc.* 130, 5022–5023. doi: 10.1021/ja711260m
- Si, W., Xin, P., Li, Z.-T., and Hou, J.-L. (2015). Tubular ubumolecular transmembrane channels: construction strategy and transport activities. *Acc. Chem. Res.* 48, 1612–1619. doi: 10.1021/acs.accounts.5b00143
- Song, N., and Yang, Y.-W. (2015). Molecular and supramolecular switches on Mesoporous silica nanoparticles. *Chem. Soc. Rev.* 44, 3474–3504. doi: 10.1039/C5CS00243E
- Strutt, N. L., Zhang, H., Giesener, M. A., Lei, J., and Stoddart, J. F. (2012). A self-complexing and self-assembling pillar[5]arene. *Chem. Comm.* 48, 1647–1649. doi: 10.1039/C2CC16030G
- Sun, S., Geng, M., Huang, L., Chen, Y., Cen, M., Lu, D., et al. (2018). A new amphiphilic pillar[5]arene: synthesis and controllable self-assembly in water and application in white-light-emitting systems. *Chem. Commun.* 54, 13006–13009. doi: 10.1039/C8CC07658H
- Wang, P., Liang, B., and Xia, D. (2019). A linear AIE supramolecular polymer based on a salicylaldehyde azine-containing pillararene and its reversible cross-linking by Cu<sup>II</sup> and cyanide. *Inorg. Chem.* 58, 2252–2256. doi: 10.1021/acs.inorgchem.8b02896
- Wang, W., Chen, L.-J., Wang, X.-Q., Sun, B., Li, X., Zhang, Y., et al. (2015). Organometallic rotaxane dendrimers with fourth-generation mechanically interlocked branches. *Proc. Natl. Acad. Sci. USA.* 112, 5597–5601. doi: 10.1073/pnas.1500489112
- Wang, X. Q., Wang, W., Li, W. J., Chen, L. J., Yao, R., Yin, G. Q. et al. (2018). Dual stimuli-responsive rotaxane-branched dendrimers with reversible dimension modulation. *Nat. Commun.* 9:3190. doi: 10.1038/s41467-018-05670-y
- Wang, Y., Ping, G., and Li, C. (2016). efficient complexation between pillar[5]arenes and neutral guests: from host-guest chemistry to functional materials. *Chem. Commun.* 52, 9858–9872. doi: 10.1039/C6CC03999E
- Wu, X., Ni, M., Xia, W., Hu, X.-Y., and Wang, L. (2015). A novel dynamic pseudo[1]rotaxane based on a mono-biotin-functionalized pillar[5]arene. *Org. Chem. Front.* 2, 1013–1017. doi: 10.1039/C5QO00159E
- Xia, B., and Xue, M. (2014). Design and efficient synthesis of a pillar[5]arene-based [1]rotaxane. *Chem. Comm.* 50, 1021–1023. doi: 10.1039/C3CC48014C
- Xiao, T., and Wang, L. (2018). Recent advances of functional gels controlled by pillar[n]arene-based host–guest interactions. *Tetrahedron Lett.* 59, 1172–1182. doi: 10.1016/j.tetlet.2018.02.028
- Xiao, T., Zhong, W., Xu, L., Sun, X.-Q., Hu, X.-Y., and Wang, L. (2019a). Supramolecular vesicles based on pillar[n]arenes: design, construction, and applications. *Org. Biomol. Chem.* 17, 1336–1350. doi: 10.1039/C8OB03095B
- Xiao, T., Zhou, L., Xu, L., Zhong, W., Zhao, W., Sun, X.-Q., et al. (2019b). Dynamic materials fabricated from water soluble pillar[n]arenes bearing triethylene oxide groups. *Chin. Chem. Lett.* 30, 271–276. doi: 10.1016/j.ccl.2018.05.039
- Xue, M., Yang, Y., Chi, X., Zhang, Z., and Huang, F. (2012). Pillararenes, a new class of macrocycles for supramolecular chemistry. *Acc. Chem. Res.* 45, 1294–1308. doi: 10.1021/ar2003418
- Yonath, A. (2010). Hibernating bears, antibiotics, and the evolving ribosome. *Angew. Chem.* 49, 4340–4354. doi: 10.1002/anie.201001297
- Yoo, C., Dodge, H. M., and Miller, A. J. M. (2019). Cation-controlled catalysis with crown ether-containing transition metal complexes. *Chem. Comm.* 55, 5047–5059. doi: 10.1039/C9CC00803A
- Zhang, H., Zhou, B., Li, H., Qu, D.-H., and Tian, H. (2013). A ferrocene-functionalized [2]rotaxane with fluorophores as stoppers. *J. Org. Chem.* 78, 2091–2098. doi: 10.1021/jo302107a
- Zhang, Z.-J., Zhang, H.-Y., Wang, H., and Liu, Y. (2011). A twin-axial hetero[7]rotaxane. *Angew. Chem.* 50, 10834–10839. doi: 10.1002/anie.201105375
- Zhu, X.-Z., and Chen, C.-F. (2005). A highly efficient approach to [4]pseudocatenanes by threefold metathesis reactions of a triptycene-based tris[2]pseudorotaxane. *J. Am. Chem. Soc.* 127, 13158–13159. doi: 10.1021/ja0546020

**Conflict of Interest Statement:** The authors declare that the research was conducted in the absence of any commercial or financial relationships that could be construed as a potential conflict of interest.

Copyright © 2019 Zhang, Wang, Long, Chen, Yan and Yao. This is an open-access article distributed under the terms of the Creative Commons Attribution License (CC BY). The use, distribution or reproduction in other forums is permitted, provided the original author(s) and the copyright owner(s) are credited and that the original publication in this journal is cited, in accordance with accepted academic practice. No use, distribution or reproduction is permitted which does not comply with these terms.